Modeling Earth Systems and Environment
https://doi.org/10.1007/s40808-022-01607-z

ORIGINAL ARTICLE

Modeling and optimal control of monkeypox with cost-effective strategies

Olumuyiwa James Peter[1,2] · Chinwendu E. Madubueze[3] · Mayowa M. Ojo[4,5] · Festus Abiodun Oguntolu[6] · Tawakalt Abosede Ayoola[7]

Received: 29 September 2022 / Accepted: 7 November 2022

Abstract

In this work, we develop and analyze a deterministic mathematical model to investigate the dynamics of monkeypox. We examine the local and global stability of the basic model without control variables. The outcome demonstrates that when the reproduction number $\mathcal{R}_0 < 1$, the model's disease-free equilibrium would be locally and globally asymptotically stable. We further analyze the effective control of monkeypox in a given population by formulating and analyzing an optimal control problem. We extend the basic model to include four control variables, namely preventive strategies for transmission from rodents to humans, prevention of infection from human to human, isolation of infected individuals, and treatment of isolated individuals. We established the necessary conditions for the existence of optimal control using Pontryagin's maximal principle. To illustrate the impact of different control combinations on the spread of monkeypox, we use the fourth-order Runge–Kutta forward–backward sweep approach to simulate the optimality system. A cost-effectiveness study is conducted to educate the public about the most cost-effective method among various control combinations. The results suggest that, of all the combinations considered in this study, implementing preventive strategies for transmission from rodents to humans is the most economical and effective among all competing strategies.

Keywords Monkeypox · Optimal control · Cost-effectiveness · Preventive strategies · Isolation

Introduction

Monkeypox is a viral disease that causes skin lesions that look like the pox. Although it is closely linked to smallpox, it is not nearly as dangerous. Monkeypox has a recent history (1958), with medical practitioners diagnosing the first human cases and distinguishing them from smallpox in the early 1970s. Since May 2022, every continent except Antarctica has reported at least 15,000 confirmed cases of monkeypox (Bisanzio and Reithinger 2022). Monkeypox is caused by the monkeypox virus (MPXV) (Durski et al. 2018; Jezek et al. 1988). The majority of infections are spread via direct contact between animals (rodents) and humans. Monkeypox is a severe disease caused by the monkeypox virus, which is similar to smallpox. It is usually found in Africa, although it is also been seen in other parts of the world. Fever and chills are common symptoms of monkeypox, and a rash appears within a few days. The monkeypox virus is contagious in a variety of animal species. The natural history of the monkeypox virus is still unknown, and further research

✉ Olumuyiwa James Peter
peterjames4real@gmail.com

1 Department of Mathematical and Computer Sciences, University of Medical Sciences, Ondo City, Ondo State, Nigeria

2 Department of Epidemiology and Biostatistics, School of Public Health, University of Medical Sciences, Ondo City, Ondo State, Nigeria

3 Department of Mathematics, Federal University of Agriculture, Makurdi, Benue State, Nigeria

4 Thermo Fisher Scientific, Microbiology Division, Lenexa, KS, USA

5 Department of Mathematical Sciences, University of South Africa, Florida, South Africa

6 Department of Mathematics, Federal University of Technology, Minna, Niger State, Nigeria

7 Department of Mathematical Sciences, Osun State University, Osogbo, Osun State, Nigeria

Published online: 22 November 2022

is needed to determine the specific reservoir(s) and how virus circulation is maintained in nature. A possible risk factor is eating undercooked meat and other animal products from infected animals (Alakunle et al. 2020). In non-endemic nations that have found cases, more public health investigations are underway, including intensive case detection and contact tracing, laboratory analysis, clinical management, and isolation with supportive care. Genomic sequencing has been used to identify the monkeypox viral clade(s) in this outbreak, where possible. Although there are no specific treatments for monkeypox infection at present time, however, the outbreaks can be controlled.

Monkeypox outbreak can be controlled with the smallpox vaccine, Cidofovir, ST-246, but the vaccination is not yet available because smallpox has been eradicated globally and also with antivirals medication such as tecovirimat, Cidofovir and Brincidofovir developed for use in patients with smallpox may prove beneficial against monkeypox (Center 2022). The best available information about the benefits and dangers of smallpox vaccination and medicine used for the prevention and management of monkeypox and other orthopoxvirus infections was used to establish Centers for Disease Control and Prevention (CDC) guidance. Many researchers have utilized mathematical models to study the epidemiology of diseases in different populations, and they have proven to be an effective and useful tool. To gain a better knowledge of the disease's transmission dynamics and control, many models have been developed and studied using various methodologies. These studies include the following: Peter et al. (2018, 2020, 2021b), Ojo et al. (2018, 2021, 2022c), Abioye et al. (2018, 2021), Ojo and Goufo (2021, 2022b), Ayoola et al. (2021). In the past, monkeypox research has received little attention, which contributed to a lack of knowledge about the disease's transmission dynamics. Despite this, a few studies have attempted to use a mathematical modeling technique to understand the dynamics of the monkeypox virus. In Peter et al. (2021a), the authors proposed a deterministic mathematical model to investigate the dynamics of the monkeypox virus in the human population. The asymptotic stability conditions for disease-free and endemic equilibria are determined in both the local and global states. The model exhibits backward bifurcation, with the locally stable disease-free equilibrium coexisting with an endemic equilibrium. Furthermore, the conditions under which the model's disease-free equilibrium was found to be globally asymptotically stable. The findings suggest that isolating infected people from the general population helps to reduce disease transmission. Usman and Adamu (2017) investigated the dynamics of the monkeypox virus in human hosts and rodents using stability analysis. A sensitivity analysis was performed on the model parameters, which revealed that the basic reproduction numbers of the model, which served as a threshold for measuring new infections in host populations decreased as the control parameters of vaccination and treatment were increased.

According to Bhunu and Mushayabasa (2011), the basis for transmission analysis of pox-like dynamics of monkeypox virus as a case study was examined, and the numerical simulations suggest that people's immune status varies the way they recover after infection with the orthopoxvirus. The authors of Bhunu et al. (2009) demonstrated that with the planned treatment intervention, the disease will be eradicated from both human and non-human primates in due course. In Lasisi et al. (2020), the authors presented a mathematical model of monkeypox transmission based on an ordinary differential equation to analyze the disease's dynamics. The solutions were found to be positive throughout the model's feasible region. The model's disease-free equilibrium and effective basic reproduction number were investigated. Other notable contributions include TeWinkel (2019), Emeka et al. (2018), Somma et al. (2019), Bankuru et al. (2020) and Grant et al. (2020). By taking into account different situations, each of the aforementioned investigations reveals a significant finding for monkeypox dynamics. However, we observed that no study has yet been conducted to investigate the dynamics of monkeypox using an optimal control approach and a cost-effectiveness analysis of the control strategies. Because of the above, we developed a deterministic mathematical model to analyze the dynamics of monkeypox while employing the most cost-effective control measures. The rest of the paper is structured as follows: the next section deals with the model formulation, the third section deals with the analysis of the basic model, the fourth section deals with the analysis of the control model, while the fifth section is the numerical simulations of the optimal control model. In the sixth section, the cost-effectiveness analysis of the optimal control model is presented, while the conclusion and recommendation of the study is given in the last section.

Methods

We formulate a deterministic model of the monkeypox virus by considering two populations, humans and rodents. The human population is sub-divided into five compartments based on the epidemiological status of individuals in the population. The compartments are, susceptible humans S_h, exposed humans E_h, infected humans I_h, isolated humans J_h

and recovered human R_h. Furthermore, the rodent population is further sub-divided into susceptible rats S_r and infected rats I_r. The total population of human and rodent population with respect to time is given as $N_h(t)=S_h + E_h + I_h + J_h + R_h$ and $N_r(t)= S_r + I_r$, respectively. The susceptible human population is increased through birth or immigration at a constant recruitment rate θ_h, and the population of the susceptible class is reduced after effective interaction with infected individuals at the rate

$$\alpha_1 = \frac{\alpha_r I_r + \alpha_h (I_h + \theta_m J_h)}{N_h},$$

where α_r and α_h represent the rate of transmission per contact with infected humans and rat, respectively. Individuals who have been infected in the susceptible class become exposed. In this state, individuals go through an infection incubation period before becoming infectious and then advance through the infectious class at a rate τ. The parameter k represents the isolation rate due to surveillance or contact tracing, while the natural recovery rate of individuals in the infected class and recovery of individuals in the isolated class through treatment is represented by ρ. θ is the modification parameter for the recovery rate of individuals in the infected class while θ_m represents the modification parameter for disease transmission for individuals in isolation. We assume that the human and rat population decreased by a natural death at the rate of μ_h and μ_r, respectively. The disease-induced death is at a rate δ_h, the population of the rat population is increased at a constant rate θ_r while the sub-population of the rodent is decreased as a result of effective contact with the rodent at a rate α_2 which is expressed as

$$\alpha_2 = \frac{\alpha_r I_r}{N_r},$$

where α_r is the transmission rate per contact with the infected rats. The descriptions above can be illustrated in a system of differential equations in (1), while the model's compartmental flow diagram is shown in Fig. 1:

$$\begin{aligned}
\frac{dS_h}{dt} &= \theta_h - \alpha_1 S_h - \mu_h S_h,\\
\frac{dE_h}{dt} &= \alpha_1 S_h - (\tau + \mu_h) E_h,\\
\frac{dI_h}{dt} &= \tau E_h - (\mu_h + \delta_h) I_h - (k + \theta\rho) I_h,\\
\frac{dJ_h}{dt} &= k I_h - (\rho + \mu_h) J_h,\\
\frac{dR_h}{dt} &= \theta\rho I_h + \rho J_h - \mu_R,\\
\frac{dS_r}{dt} &= \theta_r - \alpha_2 S_r - \mu_r S_r,\\
\frac{dI_r}{dt} &= \alpha_2 S_r - \mu_r I_r.
\end{aligned} \tag{1}$$

Table 1 Description of the model variables

Variable	Description
$S_h(t)$	Susceptible humans
$E_h(t)$	Exposed humans
$I_h(t)$	Infected humans
$J_h(t)$	Isolated humans
$R_h(t)$	Recovered humans
$S_r(t)$	Susceptible rodents
$I_r(t)$	Infected rodents

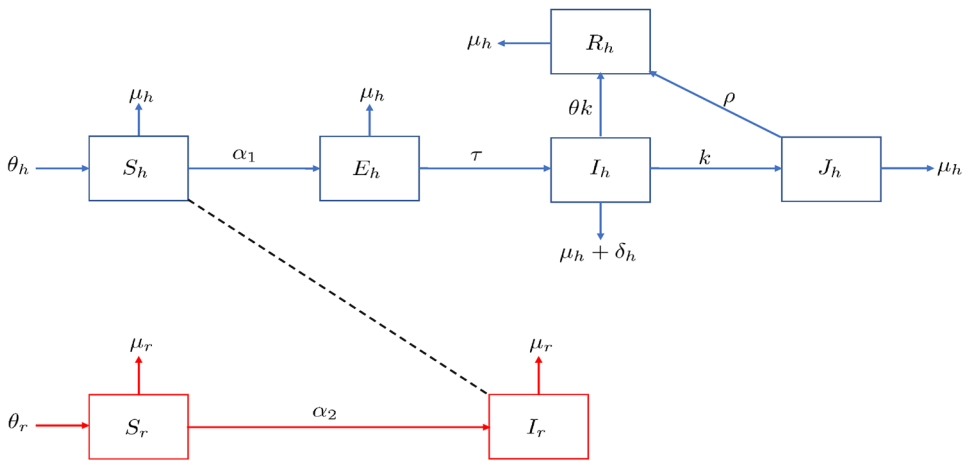

Fig. 1 Flow chart of the monkeypox model (1)

Model analysis

Invariant region

In this section, we analyzed the model (1) in the epidemiological domain as follows. Consider the epidemiological region such that, $\psi = \psi_h\ \psi_r \in \mathbb{R}_+^5\ \mathbb{R}_+^2$, such that

$$\psi_h = \left\{ (S_h, E_h, I_h, J_h, R_h) \in \mathbb{R}_+^5 : N_h \leq \frac{\theta_h}{\mu_h} \right\}. \tag{2}$$

and

$$\psi_r = \left\{ (S_r, I_r) \in \mathbb{R}_+^2 : N_r \leq \frac{\theta_r}{\mu_r} \right\}. \tag{3}$$

We can demonstrate that the set ψ is a non-negative invariant set and global attractor of this system. This means that any phase trajectory initiated anywhere in the non-negative region $\mathbb{R}_+^7$ enters the feasible region ψ and remains in ψ thereafter.

Lemma 1

The region $\psi \subset \mathbb{R}_+^7$ is non-negatively invariant of the monkeypox model (1) with non-negative initial conditions $\mathbb{R}_+^7$.

Proof Let ψ represents the feasible region of the monkeypox model (1), expressed as

$$\psi \subset \mathbb{R}_+^7.$$

Next, we show the conditions for the positive invariance of ψ that is, the solution in ψ remains in $\psi\ \forall\, t > 0$. We obtain this by adding (1) for the two populations (i.e., humans and rodents population).

$$\frac{dN_h(t)}{dt} \leq \theta_h - \mu_h N_h(t)$$

and

$$\frac{dN_r(t)}{dt} \leq \theta_r - \mu_r N_r(t).$$

Using the standard comparison theorem (Choi et al. 2014), we can say that

$$\begin{aligned} N_h(t) &\leq N_h(0)e^{-\mu_h t} + \frac{\theta_h}{\mu_h}\left(1 - e^{-\mu_h t}\right) \quad \text{and} \\ N_r(t) &\leq N_r(0)e^{-\mu_r t} + \frac{\theta_r}{\mu_r}\left(1 - e^{-\mu_r t}\right). \end{aligned} \tag{4}$$

Particularly, $N_h(t) \leq \frac{\theta_h}{\mu_h}$ if $N_h(0) \leq \frac{\theta_h}{\mu_h}$. Also, $N_r(t) \leq \frac{\theta_r}{\mu_r}$ if $N_r(0) \leq \frac{\theta_r}{\mu_r}$. Therefore, the region ψ is a non-negative invariant. □

Existence and stability of the monkeypox free equilibrium

Disease-free equilibrium is the equilibrium state in the absence of the disease. This is obtained by setting the right hand side of (1), and variables I_h and J_h to zero. Hence, the disease-free equilibrium state is given by

$$\mathcal{E}_0 = (S_h^0, E_h^0, I_h^0, J_h^0, R_h^0, S_r^0, I_r^0) = \left(\frac{\theta_h}{\mu_h}, 0, 0, 0, 0, \frac{\theta_r}{\mu_r}, 0\right). \tag{5}$$

We also obtain the reproduction number as a threshold quantity to investigate the system's stability. This is accomplished by employing the method in Peter et al. (2022) called the next generation matrix. The Jacobian matrices of F_i and V_i at the disease-free equilibrium are given by

$$F = \begin{bmatrix} 0 & \alpha_h & \alpha_h\theta_m & \alpha_b \\ 0 & 0 & 0 & 0 \\ 0 & 0 & 0 & 0 \\ 0 & 0 & 0 & \alpha_r \end{bmatrix} \text{ and } V = \begin{bmatrix} f_1 & 0 & 0 & 0 \\ -\tau & f_2 & 0 & 0 \\ 0 & -k & f_3 & 0 \\ 0 & 0 & 0 & \mu_r \end{bmatrix},$$

where $f_1 = \tau + \mu_h$, $f_2 = \mu_h + \delta_h + k + \theta\rho$, and $f_3 = \rho + \mu_h$. The basic reproduction number, $\mathcal{R}_0$ is the spectral radius of the matrix FV^{-1} given by

$$\mathcal{R}_0 = \max(\mathcal{R}_r, \mathcal{R}_h) = \max\left(\frac{\alpha_r}{\mu_r}, \frac{\alpha_h \tau k \theta_m}{f_1 f_2 f_3} + \frac{\alpha_h \tau}{f_1 f_2}\right), \tag{6}$$

where $\mathcal{R}_r = \frac{\alpha_r}{\mu_r}$ is the rodent reproduction number while $\mathcal{R}_h = \mathcal{R}_{hi} + \mathcal{R}_{hj}$ is reproduction number for human to human with $\mathcal{R}_{hi} = \frac{\alpha_h \tau k \theta_m}{f_1 f_2 f_3}$ and $\mathcal{R}_{hj} = \frac{\alpha_h \tau}{f_1 f_2}$ as the respective reproduction numbers from infected and isolated human to susceptible human.

Local stability of the disease-free equilibrium

Theorem 1 *The monkeypox -free equilibrium ε_0, of the model (1) is locally asymptotically stable in the biological feasible region if $\mathcal{R}_0 < 1$ and unstable if $\mathcal{R}_0 > 1$.*

The local stability of the disease-free equilibrium is established using the linearization method. The Jacobian matrix of the model (1) at disease-free equilibrium is given by

$$\mathcal{J}(\mathcal{E}_0) = \begin{vmatrix} -\mu_h & 0 & -\alpha_h & -\alpha_h\theta_m & 0 & 0 & -\alpha_b \\ 0 & -f_1 & \alpha_h & \alpha_h\theta_m & 0 & 0 & \alpha_b \\ 0 & \tau & -f_2 & 0 & 0 & 0 & 0 \\ 0 & 0 & k & -f_3 & 0 & 0 & 0 \\ 0 & 0 & \rho\phi & \rho & -\mu_h & 0 & 0 \\ 0 & 0 & 0 & 0 & 0 & -\mu_r & -\alpha_r \\ 0 & 0 & 0 & 0 & 0 & 0 & \alpha_r - \mu_r \end{vmatrix}. \tag{7}$$

The eigenvalues of $\mathcal{J}(\mathcal{E}_0)$ are $\alpha_r - \mu_r = \mu_r(\mathcal{R}_r - 1), -\mu_r, -\mu_h$ twice and the roots of the polynomial

$$a_0\lambda^3 + a_1\lambda^2 + a_2\lambda + a_3 = 0, \tag{8}$$

where $a_0 = 1$, $a_1 = f_1 + f_2 + f_3$, $a_2 = f_1f_3 + f_2f_3 + f_1f_2(1 - \mathcal{R}_{hj})$, and $a_3 = f_1f_2f_3(1 - \mathcal{R}_h)$.

Using Routh–Hurwitz criteria, the polynomial (8) has negative real roots if $a_0 > 0$, $a_1 > 0$, $a_2 > 0$, $a_3 > 0$ and $a_1a_2 - a_0a_3 > 0$. This is true since $a_1a_2 - a_0a_3 > 0 = a_1(f_1 + f_2) - f_1f_2f_3\mathcal{R}_{hi}$. Thus, the eigenvalues of $\mathcal{J}(\mathcal{E}_0)$ are all negative if $\mathcal{R}_0 = \max(\mathcal{R}_r, \mathcal{R}_h) < 1$. This implies that the disease-free equilibrium, $\mathcal{E}_0$ is locally asymptotically stable if $\mathcal{R}_0 < 1$. Monkeypox infection can be controlled in a population if $\mathcal{R}_0$ is less than one and the initial size of the sub-populations of the system (1) are in the basin of attraction of $\mathcal{E}_0$. Above is the brief illustration of Theorem 1.

Optimal control model

We extend the monkeypox model in (1) by incorporating four time-dependent control variables namely; preventive strategies for transmission from rodents to humans u_1, prevention from human-to-human contact u_2, isolation of infected individuals through contact tracing u_3, and treatment of isolated individuals u_4. By introducing the above control interventions, we have the following system of equations:

$$\begin{aligned}
\frac{dS_h}{dt} &= \theta_h - \frac{\alpha_r I_r S_h(1-u_1(t))}{N_h} \\
&\quad - \frac{\alpha_h(I_h + J_h)S_h(1-u_2(t))}{N_h} - \mu_h S_h, \\
\frac{dE_h}{dt} &= \frac{\alpha_r I_r S_h(1-u_1(t))}{N_h} \\
&\quad + \frac{\alpha_h(I_h + J_h)S_h(1-u_2(t))}{N_h} - (\tau + \mu_h)E_h, \\
\frac{dI_h}{dt} &= \tau E_h - (\mu_h + \delta_h + u_3(t) + \theta\rho)I_h, \\
\frac{dJ_h}{dt} &= u_3(t)I_h - (u_4(t) + \mu_h)J_h, \\
\frac{dR_h}{dt} &= \theta\rho I_h + u_4(t)J_h - \mu_h R_h, \\
\frac{dS_r}{dt} &= \theta_r - \frac{\alpha_r I_r S_r}{N_r} - \mu_r S_r, \\
\frac{dI_r}{dt} &= \frac{\alpha_r I_r S_r}{N_r} - \mu_r I_r,
\end{aligned} \tag{9}$$

where $k = u_3$ and ρ=u_4 and the initial conditions $S_h \geq 0$, $E_h \geq 0$, $I_h \geq 0$, $J_h \geq 0$, $R_h \geq 0$, $S_r \geq 0$, $I_r \geq 0$.

We aim to minimize, the exposed E_h, infected I_h and isolated J_h humans and the cost involved in using the controls. According to Pontryagin (1987) and Fleming and Rishel (2012), the objective function is defined as

$$\begin{aligned}
J(u_1, u_2, u_3, u_4) = \int_0^{t_f} & \left(A_1E_h + A_2I_h + A_3J_h + B_1\frac{u_1^2}{2} \right. \\
& \left. + B_2\frac{u_2^2}{2} + B_3\frac{u_3^2}{2} + B_4\frac{u_4^2}{2} \right) dt,
\end{aligned} \tag{10}$$

where A_1, A_2, and A_3 are positive weight constant of the exposed humans, infected humans, and isolated humans, respectively. Also, the cost control functions take a quadratic form, such that $\frac{B_1u_1^2}{2}$, $\frac{B_2u_2^2}{2}$, $\frac{B_3u_3^2}{2}$, and $\frac{B_4u_4^2}{2}$ represent the cost control function for prevention from rodents to humans, prevention from human-to-human contact, isolation through contact tracing and treatment of isolated individuals, respectively. The aim is to find an optimal control of $u_1^*(t)$, $u_2^*(t)$, $u_3^*(t)$ and $u_4^*(t)$ such that

$$J(u_1^*, u_2^*, u_3^*, u_4^*) = min\{(u_1, u_2, u_3, u_4) : u_1, u_2, u_3, u_4 \in \Delta\}, \tag{11}$$

where Δ is the non-empty control subject to the optimal control model set defined as $\Delta = \{u_i : 0 \leq u_i(t) \leq 1$, Lebesgue measurable $t = [0, t_f]$ for $i = 1, 2, 3, 4\}$ represents the control set with respect with initial conditions.

Next, we show that the optimal control problem exists. The Pontryagin's Maximum Principle gives the necessary conditions for which the optimal control $u^* = (u_1, u_2, u_3, u_4)$ exists. According to Pontryagin (1987), the Hamiltonian function is given by

$$\begin{aligned}
H = {} & A_1 E_{\mathrm{h}} + A_2 I_{\mathrm{h}} + A_3 J_{\mathrm{h}} + B_1 \frac{u_1^2(t)}{2} + B_2 \frac{u_2^2(t)}{2} \\
& + B_3 \frac{u_3^2(t)}{2} + B_4 \frac{u_4^2(t)}{2} \\
& + \lambda_1 \left[\theta_{\mathrm{h}} - \frac{\alpha_{\mathrm{r}} I_{\mathrm{r}} S_{\mathrm{h}} (1 - u_1(t))}{N_{\mathrm{h}}} \right. \\
& \left. - \frac{\alpha_{\mathrm{h}} (I_{\mathrm{h}} + J_{\mathrm{h}}) S_{\mathrm{h}} (1 - u_2(t))}{N_{\mathrm{h}}} - \mu_{\mathrm{h}} S_{\mathrm{h}} \right] \\
& + \lambda_2 \left[\frac{\alpha_{\mathrm{r}} I_{\mathrm{r}} S_{\mathrm{h}} (1 - u_1(t))}{N_{\mathrm{h}}} \right. \\
& \left. + \frac{\alpha_{\mathrm{h}} (I_{\mathrm{h}} + J_{\mathrm{h}}) S_{\mathrm{h}} (1 - u_2(t))}{N_{\mathrm{h}}} - (\tau + \mu_{\mathrm{h}}) E_{\mathrm{h}} \right] \\
& + \lambda_3 [\tau E_{\mathrm{h}} - (\mu_{\mathrm{h}} + \delta_{\mathrm{h}} + u_3(t) + \theta\rho) I_{\mathrm{h}}] \\
& + \lambda_4 [u_3(t) I_{\mathrm{h}} - (u_4(t) + \mu_{\mathrm{h}}) J_{\mathrm{h}}] \\
& + \lambda_5 [\theta\rho I_{\mathrm{h}} + u_4(t) J_{\mathrm{h}} - \mu_{\mathrm{h}} R_{\mathrm{h}}] \\
& + \lambda_6 \left[\theta_{\mathrm{r}} - \frac{\alpha_{\mathrm{r}} I_{\mathrm{r}} S_{\mathrm{r}}}{N_{\mathrm{r}}} - \mu_{\mathrm{r}} S_{\mathrm{r}} \right] \\
& + \lambda_7 \left[\frac{\alpha_{\mathrm{r}} I_{\mathrm{r}} S_{\mathrm{r}}}{N_{\mathrm{r}}} - \mu_{\mathrm{r}} I_{\mathrm{r}} \right],
\end{aligned} \tag{12}$$

where $\lambda_1, \lambda_2, \lambda_3, \lambda_4, \lambda_5, \lambda_6$, and λ_7 are the adjoint variables associated with the state variables of the optimal control model in (9). Following the approach in Peter et al. (2020), Ayoola et al. (2021), and Madubueze et al. (2021), we establish the characterization result in the theorem as follows.

Theorem 2 *Let $S_{\mathrm{h}}^*, E_{\mathrm{h}}^*, I_{\mathrm{h}}^*, J_{\mathrm{h}}^*, R_{\mathrm{h}}^*, S_{\mathrm{r}}^*$, and I_{r}^* be optimal state solutions associated with optimal control u_1^*, u_2^*, u_3^*, and u_4^* for the optimal control problem in (9). There exist an adjoint functions λ_i which satisfy the system (12) with the transversality conditions $\lambda_i(t_f) = 0$ in (14) for $i = 1, 2, 3, 4$ and the control variables $(u_1^*, u_2^*, u_3^*, u_4^*)$.*

Proof By differentiating the Hamiltonian function (12) with respect to the state variables $S_{\mathrm{h}}, E_{\mathrm{h}}, I_{\mathrm{h}}, J_{\mathrm{h}}, R_{\mathrm{h}}, S_{\mathrm{r}}$ and I_{r}, we have the following: □

$$\begin{aligned}
\frac{\mathrm{d}\lambda_1}{\mathrm{d}t} = {} & -\frac{\partial H}{\partial S_{\mathrm{h}}} = (\lambda_1 - \lambda_2) \\
& \left(\frac{\alpha_{\mathrm{r}} I_{\mathrm{r}} (1 - u_1)}{N_{\mathrm{h}}} + \frac{\alpha_{\mathrm{h}} (I_{\mathrm{h}} + \theta_{\mathrm{m}} J_{\mathrm{h}}) (1 - u_2)}{N_{\mathrm{h}}} \right) \\
& \left(1 - \frac{S_{\mathrm{h}}}{N_{\mathrm{h}}} \right) + \mu_{\mathrm{h}} \lambda_1 \\
\frac{\mathrm{d}\lambda_2}{\mathrm{d}t} = {} & -\frac{\partial H}{\partial E_{\mathrm{h}}} = -A_1 + (\lambda_2 - \lambda_1) \\
& \left(\frac{\alpha_{\mathrm{r}} I_{\mathrm{r}} S_{\mathrm{h}} (1 - u_1)}{N_{\mathrm{h}}^2} + \frac{\alpha_{\mathrm{h}} (I_{\mathrm{h}} + \theta_{\mathrm{m}} J_{\mathrm{h}}) (1 - u_2) S_{\mathrm{h}}}{N_{\mathrm{h}}^2} \right) \\
& + \mu_{\mathrm{h}} \lambda_2 + (\lambda_2 - \lambda_3) \tau \\
\frac{\mathrm{d}\lambda_3}{\mathrm{d}t} = {} & -\frac{\partial H}{\partial I_{\mathrm{h}}} = -A_2 + (\lambda_2 - \lambda_1) \\
& \left(\frac{\alpha_{\mathrm{r}} I_{\mathrm{r}} S_{\mathrm{h}} (1 - u_1)}{N_{\mathrm{h}}^2} - \frac{\alpha_{\mathrm{h}} S_{\mathrm{h}} (1 - u_2)}{N_{\mathrm{h}}} \right. \\
& \left. + \frac{\alpha_{\mathrm{h}} (I_{\mathrm{h}} + \theta_{\mathrm{m}} J_{\mathrm{h}}) S_{\mathrm{h}} (1 - u_2)}{N_{\mathrm{h}}^2} \right) \\
& + \lambda_3 + (\mu_{\mathrm{h}} + \delta_{\mathrm{h}}) + (\lambda_3 - \lambda_4) u_3 + (\lambda_3 - \lambda_5) \theta\rho \\
\frac{\mathrm{d}\lambda_4}{\mathrm{d}t} = {} & -\frac{\partial H}{\partial J_{\mathrm{h}}} = -A_3 + (\lambda_2 - \lambda_1) \\
& \left(\frac{\alpha_{\mathrm{r}} I_{\mathrm{r}} S_{\mathrm{h}} (1 - u_1)}{N_{\mathrm{h}}^2} - \frac{\alpha_{\mathrm{h}} \theta_{\mathrm{m}} S_{\mathrm{h}} (1 - u_2)}{N_{\mathrm{h}}} \right. \\
& \left. + \frac{\alpha_{\mathrm{h}} (I_{\mathrm{h}} + \theta_{\mathrm{m}} J_{\mathrm{h}}) S_{\mathrm{h}} (1 - u_2)}{N_{\mathrm{h}}^2} \right) \\
& + (\lambda_4 - \lambda_5) u_4 + \lambda_4 \mu_{\mathrm{h}} \\
\frac{\mathrm{d}\lambda_5}{\mathrm{d}t} = {} & -\frac{\partial H}{\partial R_{\mathrm{h}}} = (\lambda_2 - \lambda_1) \\
& \left(\frac{\alpha_{\mathrm{r}} I_{\mathrm{r}} S_{\mathrm{h}} (1 - u_1)}{N_{\mathrm{h}}^2} + \frac{\alpha_{\mathrm{h}} (I_{\mathrm{h}} + \theta_{\mathrm{m}} J_{\mathrm{h}}) S_{\mathrm{h}} (1 - u_2)}{N_{\mathrm{h}}^2} \right) \lambda_5 \mu_{\mathrm{h}} \\
\frac{\mathrm{d}\lambda_6}{\mathrm{d}t} = {} & -\frac{\partial H}{\partial S_{\mathrm{r}}} = (\lambda_6 - \lambda_7) \frac{\alpha_{\mathrm{r}} I_{\mathrm{r}}}{N_{\mathrm{r}}} \left(1 - \frac{S_{\mathrm{r}}}{N_{\mathrm{r}}} \right) + \mu_{\mathrm{r}} \lambda_6 \\
\frac{\mathrm{d}\lambda_7}{\mathrm{d}t} = {} & -\frac{\partial H}{\partial I_{\mathrm{r}}} = (\lambda_1 - \lambda_2) \frac{\alpha_{\mathrm{r}} S_{\mathrm{h}} (1 - u_1)}{N_{\mathrm{h}}} \left(1 - \frac{S_{\mathrm{r}}}{N_{\mathrm{r}}} \right) \\
& + (\lambda_6 - \lambda_7) \frac{\alpha_{\mathrm{r}} S_{\mathrm{r}}}{N_{\mathrm{r}}} \left(1 - \frac{I_{\mathrm{r}}}{N_{\mathrm{r}}} \right) + \mu_{\mathrm{r}} + \lambda_7
\end{aligned} \tag{13}$$

with the transversality conditions

$$\begin{aligned}
\lambda_1(t_f) = {} & \lambda_2(t_f) = \lambda_3(t_f) = \lambda_4(t_f) \\
& = \lambda_5(t_f) = \lambda_6(t_f) = \lambda_7(t_f) = 0.
\end{aligned} \tag{14}$$

To establish the optimal control of the control variable set, where $u_i = (0, 1)$, we differentiate the Hamiltonian H in (12) with respect to control variable u_1, u_2, and u_4 to obtain

$$\begin{aligned}
&\frac{\partial H}{\partial u_1} = B_1 u_1 + \lambda_1 \frac{\alpha_r I_r S_h}{N_h} - \lambda_2 \frac{\alpha_r I_r S_h}{N_h} = 0\\
&\Rightarrow u_1^* = \frac{(\lambda_2 - \lambda_1)\alpha_r I_r S_h}{B_1 N_h}\\
&\frac{\partial H}{\partial u_2} = B_2 u_2 + \frac{\lambda_1 \alpha_h (I_h + \theta_m J_h) S_h}{N_h} - \frac{\lambda_2 \alpha_h (I_h + \theta_m J_h) S_h}{N_h} = 0\\
&\Rightarrow u_2^* = \frac{(\lambda_2 - \lambda_1)\alpha_h (I_h + \theta_m J_h) S_h}{B_2 N_h}\\
&\frac{\partial H}{\partial u_3} = -\lambda_3 I_h + \lambda_4 I_h + B_3 u_3 = 0\\
&\Rightarrow u_3^* = \frac{(\lambda_3 - \lambda_4) I_h}{B_3}\\
&\frac{\partial H}{\partial u_4} = B_4 u_4 - \lambda_4 J_h + \lambda_5 J_h = 0\\
&\Rightarrow u_4^* = \frac{(\lambda_4 - \lambda_5) J_h}{B_4}.
\end{aligned} \tag{15}$$

Hence,

$$\begin{aligned}
u_1^* &= \max\left\{0, min\left(\frac{(\lambda_2 - \lambda_1)\alpha_r I_r S_h}{B_1 N_h}\right)\right\},\\
u_2^* &= \max\left\{0, min\left(\frac{(\lambda_2 - \lambda_1)\alpha_h (I_h + \theta_m J_h) S_h}{B_2 N_h}\right)\right\},\\
u_3^* &= \max\left\{0, min\left(\frac{(\lambda_3 - \lambda_4) I_h}{B_3}\right)\right\},\\
u_4^* &= \max\left\{0, min\left(\frac{(\lambda_4 - \lambda_5) J_h}{B_4}\right)\right\}.
\end{aligned} \tag{16}$$

Numerical simulations of the optimal control model

The impact of various optimum control strategies on the reduction of monkeypox prevalence in the human population is examined in this section. We specifically want to look at the impact of various combined control measures that can help quickly stop the spread of the disease in the absence of mass vaccination for monkeypox prevention. We will also investigate the most cost-effective strategy that will be suitable for use among all the various combinations of the control strategy because disease control and eradication in a large population can be difficult and expensive. This is a crucial aspect to consider when putting intervention strategies into practice, especially in developing and low-income nations.

In order to describe the dynamical behavior of a given system over time and for different parameter values and conditions, numerical simulation has shown to be a useful tool. To determine the effect of various intervention techniques on the ideal control model, we thus simulate the impact of various combinations of measures on the control of monkeypox in a given population. To do this, we use Matlab's Runge–Kutta forward–backward sweep method. We simulate the impact of seven distinct optimal control strategies on the infected human and isolated human populations. The simulation's initial conditions were taken from Peter et al. (2022), while Table 2 contains the parameter values that were used. In order to ensure that none of the three terms is dominant during simulation, we assume that the positive weight constants in the objective functions are equal such that $A_1 = A_2 = A_3 = 1$. In contrast, we assume that the weight constants relating to the overall

Table 2 Model parameter values and description

Parameter	Description	Value	Source
Λ_h	Recruitment rate of susceptible humans	64850	Peter et al. (2022)
Λ_r	Recruitment rate of rodents	0.2000	Peter et al. (2022)
μ_h	Per capita natural death rate in human	0.000303	Peter et al. (2022)
μ_r	Per capita natural death rate in rodent	0.00200	Peter et al. (2022)
α_1	Effective contact rate of rodents to humans	0.052466	Peter et al. (2022)
α_2	Effective contact rate of humans to humans	0.022325	Peter et al. (2022)
θ	Movement rate from exposed class	0.016744	Peter et al. (2022)
ρ	Fraction of individuals not detected with the virus after quarantine	$0 < \rho < 1$	Assumed
ϕ	Movement rate from quarantine	0.003286	Peter et al. (2022)
ω	Movement rate from infected class	0.088366	Peter et al. (2022)
τ	Recovery rate of individuals in the isolated class due to treatment	0.036246	Peter et al. (2022)
δ_h	Disease-induced death rate for humans	0.003286	Peter et al. (2022)
k	Fraction of exposed individuals that are quarantined	$0 < k < 1$	Assumed
α_3	Effective contact rate of rodents to rodents	0.012458	Peter et al. (2022)
γ	Fraction of infected individuals that are isolated	$0 < \gamma < 1$	Assumed

costs of control implementation are unequal. Due to the assumption that the weight constant for calculating the total cost to apply isolation through contact tracing and treat isolated individuals is higher than other controls, the weight constants are set to $B_1 = B_2 = 10$ and $B_3 = B_4 = 15$, respectively. For instance, the cost of implementing preventive strategies for transmission of infection from rodents to humans (like personal hygiene) would be lesser than the cost of isolating infected people. It is important to remember that the weight constant values chosen are based on assumptions, and they could affect how realistically the control terms behave. The cost of control, in particular, can fluctuate over time in different parts of the country; as a result, in such a situation, the weight constant will be modeled using the region's scenario. For instance, the cost of treating a patient who is separated from medical services may vary based on the severity of the infection and the cost of travel to a facility.

Table 3 Possible scenarios with their combination strategies

Scenarios	Strategies	Scenarios	Strategies
Single control	$u_1 \neq 0$	Triple controls	$u_1, u_3, u_4 \neq 0$
A	$u_2 \neq 0$	C	$u_2, u_3, u_4 \neq 0$
Double controls	$u_1, u_2 \neq 0$	Quadruplet controls	$u_1, u_2, u_3, u_4 \neq 0$
B	$u_3, u_4 \neq 0$	D	

The impact of the four optimal control techniques and their various combinations was discussed in the following sub-sections. We observe that the four distinct scenarios namely; single control, double controls, triple controls, and quadruplet controls are used to group the seven potential control strategies that were simulated in this study. Scenario A, scenario B, scenario C, and scenario D, respectively, were used to identify them. According to Table 3, each scenario is further divided into various strategies. For instance, the single control (scenario A) includes two distinct prevention methods, namely preventive strategies for transmission of infection from rodents to humans only ($u_1 \neq 0$) and prevention from human-to-human contact only ($u_2 \neq 0$).

Strategy 1: the optimal use of preventive strategies for transmission from rodents to humans only

Figure 2 depicts the effect of the optimal use of preventive strategies for transmission from rodents to humans only on

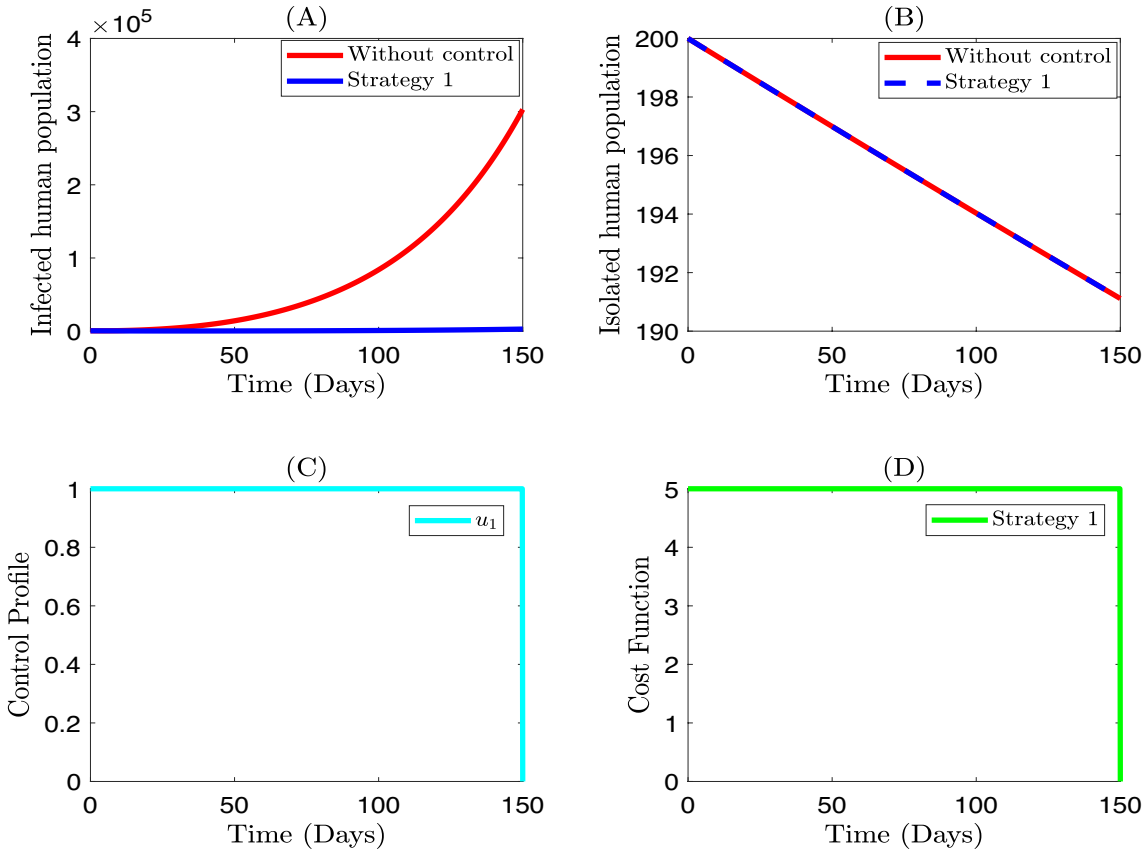

Fig. 2 Simulations of the effects of strategy 1 on the optimal control model. **A** Infected human population; **B** isolated human population; **C** control profile; and **D** cost function

the isolated and infected human population. We also show the intervention's control profile and the associated cost function necessary for the intervention's successful effects on the human population. As shown in Fig. 2A, we observed a significant decline in the number of infected people when preventive strategies for transmission from rodents to humans are practiced to their fullest. Since the application of these strategies is used in reducing the transmission of infections to susceptible people, this outcome was largely anticipated. Some studies have shown the effectiveness of preventive interventions on some infectious diseases (Ojo et al. 2022a, b), and this intervention strategy has been recommended by the Centers for Disease Control and Prevention (CDC) to reduce monkeypox spreads particularly during this insurgence (Centers for Disease Control and Prevention 2022a). This intervention averted a total size of 7.26×10^7 infected individuals. However, as shown in Fig. 2B, it is important to note that using preventive strategies for transmission from rodents to humans has no appreciable impact on the isolated human population. Since isolated humans are already contagious, interventions like treatment are more crucial in reducing the number of infected individuals than preventive measures like personal hygiene. We display the control profile of the best use of preventive strategies from rodents to humans only in Fig. 2C. The outcome demonstrates that the best use of preventive strategies for transmission from rodents to humans is maintained at the highest coverage (100%) throughout the intervention (150 days). This suggests to the public that the control effort should be implemented and maintained at its highest level throughout the intervention period in order to achieve the expected outcome of the impact of the strategy as shown in Fig. 2A. In Fig. 2D, the cost function for the ideal application of preventive strategies for transmission from rodents to humans is shown.

Strategy 2: the optimal use of prevention from human-to-human only

We show the impact of the best use of human-to-human transmission prevention u_2 only on the isolated and infected human population in Fig. 3. We also display the intervention's control profile and the related cost function necessary for the intervention's successful effects on the human population. In the presence of the best use of prevention from human to human, as shown in

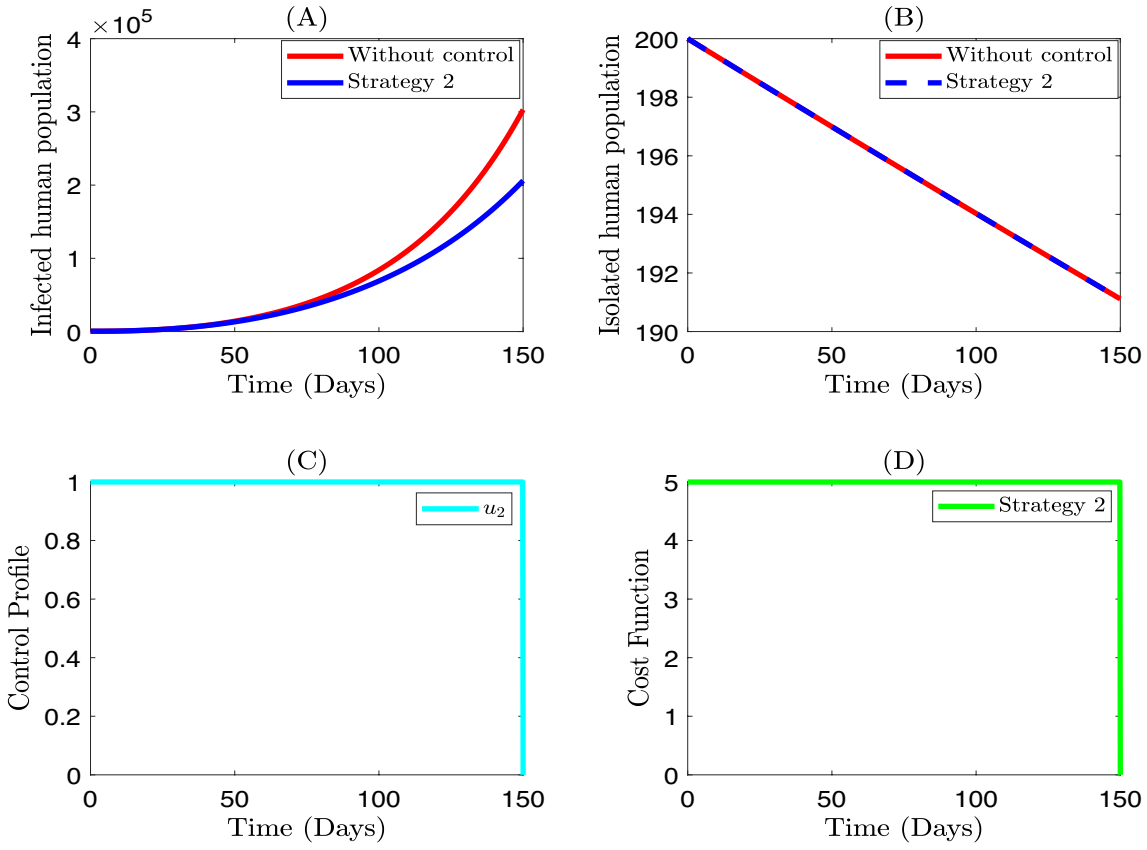

Fig. 3 Simulations of the effects of strategy 2 on the optimal control model. **A** Infected human population; **B** isolated human population; **C** control profile; and **D** cost function

Fig. 3A, we observe a minimal decrease in the population of infected humans. With this intervention, a total of 1.72×10^7 infected people were averted. It is important to note that monkeypox transmission requires the presence of a second host (a non-human). Based on this finding, it can be inferred that human-to-human transmission of the disease contributes less to the disease's prevalence and that the intervention reduces the number of infected people. It is possible to suggest that additional control measures would be required to effectively lessen the burden of the disease on the human population. In Fig. 3B, a similar result from Fig. 2B is seen on the isolated human population. Referencing Fig. 3C, we display the control profile of the ideal application of prevention from human to human only. The outcome demonstrates that the best use of this intervention is maintained at the upper bound (100%) throughout the duration of the intervention. This suggests that in order to achieve the intervention's desired outcome, the control effort should be put into place and maintained at its highest level throughout the intervention. In Fig. 3D, the cost function for the ideal use prevention from human to human is shown.

Strategy 3: the optimal use of isolation and treatment only

The combined effect of the best use of isolation of infected individuals u_3 and treatment of isolated individuals u_4 only on the infected and isolated human population is shown in Fig. 4. During the first 146 days of the intervention, as depicted in Fig. 4A, the number of infected people decreases; however, after these days, the number of infected people increases. The relaxation of the isolation strategy, as seen in the control profile shown in Fig. 4C, makes this dynamic possible. This suggests that there is a chance for an increase in infection prevalence if the practice of isolating monkeypox-infected people is discontinued. With this intervention, a total of 6.50×10^7 infected people were avoided. This finding suggests that both interventions should be maintained at their highest coverage levels in order to limit the spread of monkeypox among the general population. The impact of isolating the infected individuals and treatment of isolated people on the isolated humans is shown in Fig. 4B. We see that the size of the isolated human population increases until the optimal control intervention of isolation through contact tracing u_3 is relaxed. The cost

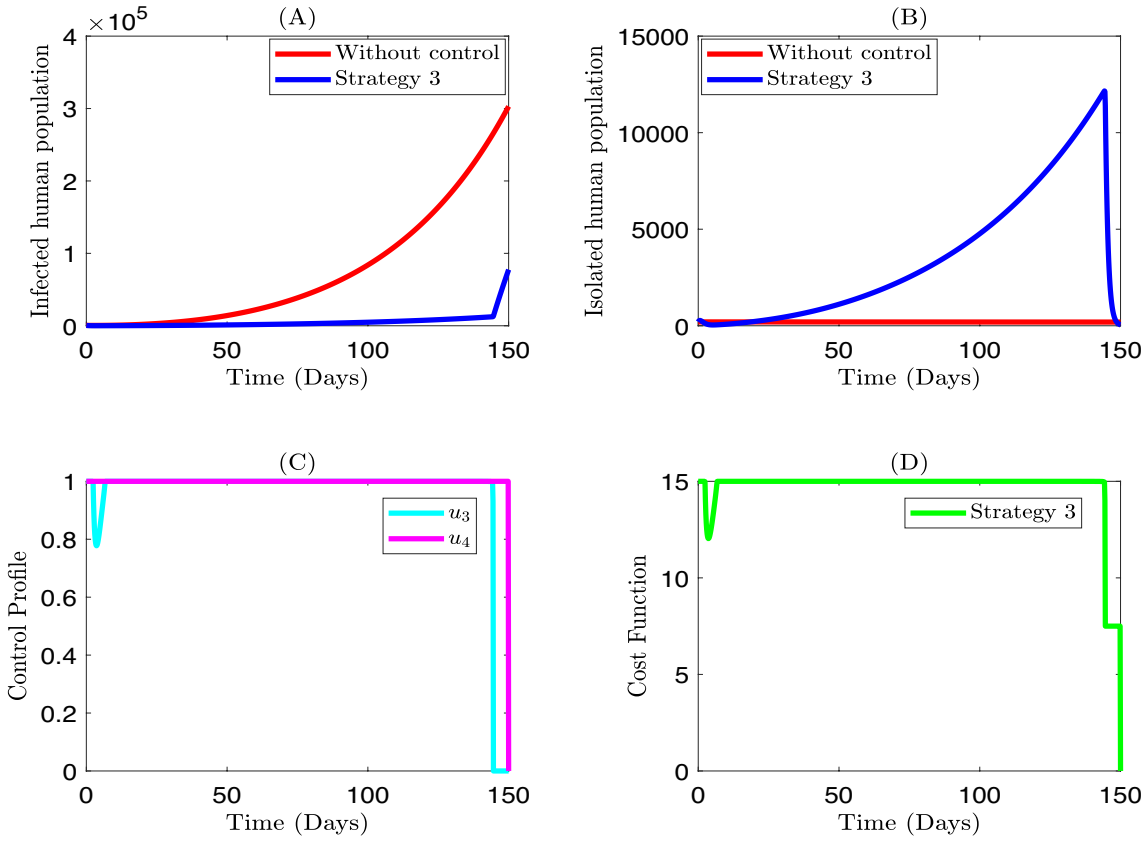

Fig. 4 Simulations of the effects of strategy 3 on the optimal control model. **A** Infected human population; **B** isolated human population; **C** control profile; and **D** cost function

function of the combined interventions (strategy 3) is shown in Fig. 4D.

Strategy 4: the optimal use of preventive strategies for transmission from rodents to humans and prevention from human-to-human only

The combined effect of preventive strategies for transmission from rodents to humans u_1 and prevention from human-to-human u_2 only on the infected and isolated human population is depicted in Fig. 5A, B, respectively with control profile in Fig. 5C. The result of this combined interventions are similar to the result presented in Fig. 2 (see Sect. 5.1). However, it is worth noting that this intervention (strategy 4) averted a total size of 7.33×10^7 infected individuals. The cost function of the combined interventions is shown in Fig. 5D.

Strategy 5: the optimal use of preventive strategies from rodents to humans, isolation, and treatment only

In Fig. 6, we demonstrate the simulation of the triple combination of the optimal use of preventive strategies from rodents to humans u_1, isolation u_3 and treatment u_4 only on the infected human and isolated human population. Throughout interventions, the infected human population declined tremendously when the combined interventions are implemented compared to the case without control as seen in Fig. 6A. These combined interventions averted a total size of 7.37×10^7 infected individuals. The size of the isolated individual's population declined in the early days of the implementation of control interventions as seen in Fig. 6B. This decline is likely a result of the relaxation of the optimal isolation intervention as depicted in Fig. 6C. The control profile shows that the optimal use of preventive strategies from rodents to humans u_1 and treatment of isolated individuals u_4 are kept at the upper bound throughout the time of intervention. This advises the public that to attain the expected outcome of the intervention (strategy 5) as shown in Fig. 6A, at least both preventive strategies from rodents to humans and treatment of isolated individuals interventions must be implemented and remain at their maximum level throughout the intervention period. The cost function for the triple interventions (strategy 5) is shown in Fig. 6D.

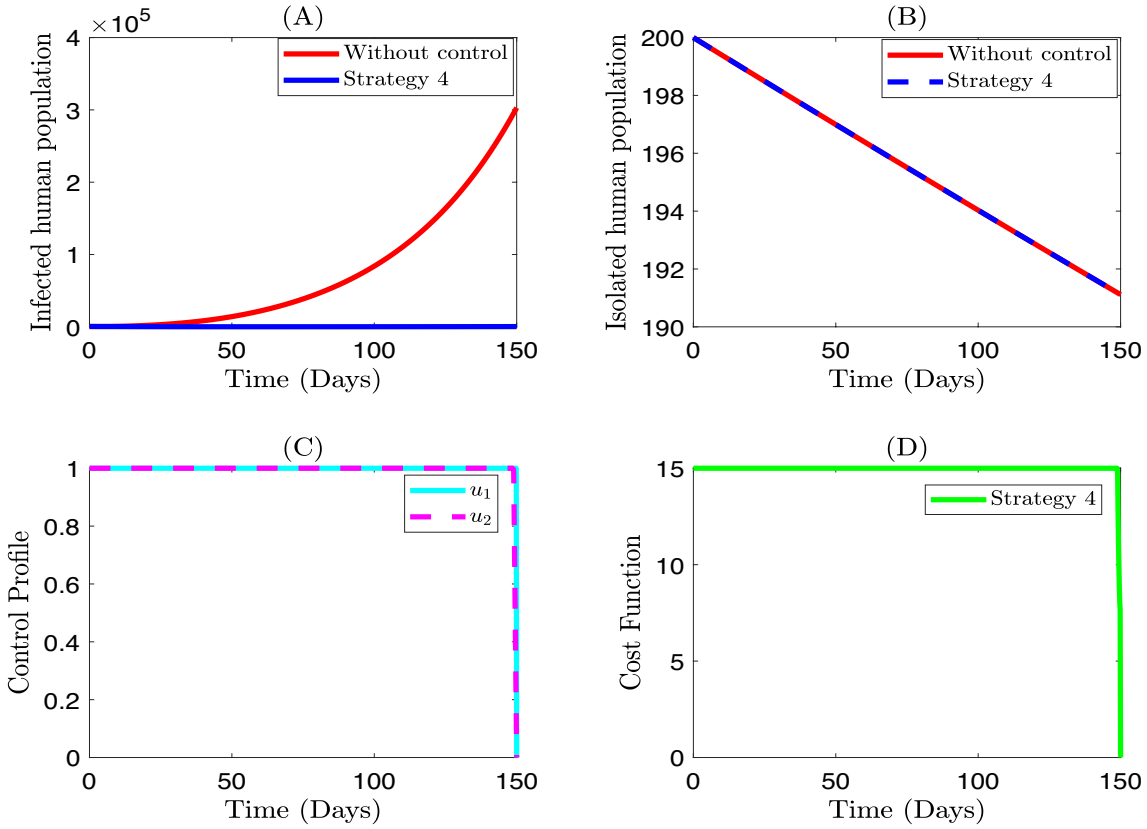

Fig. 5 Simulations of the effects of strategy 4 on the optimal control model. **A** Infected human population; **B** isolated human population; **C** control profile; and **D** cost function

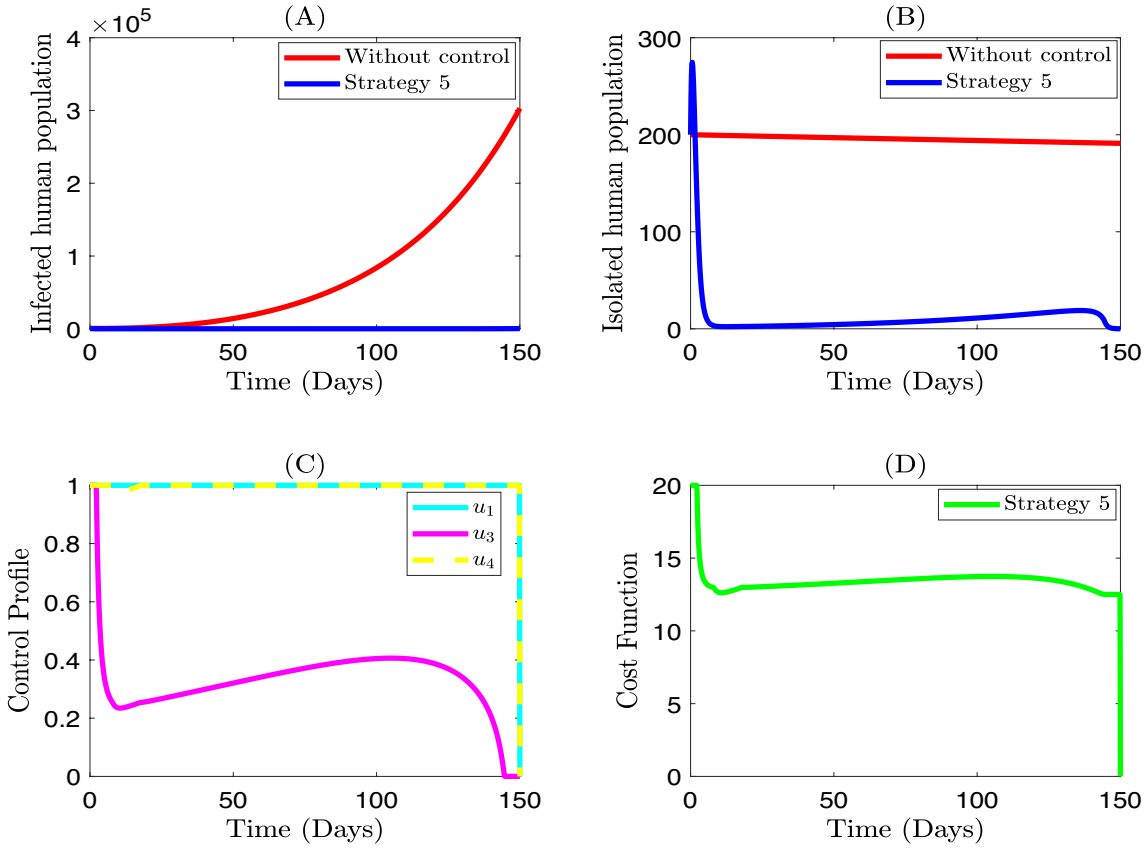

Fig. 6 Simulations of the effects of strategy 5 on the optimal control model. **A** Infected human population; **B** isolated human population; **C** control profile; and **D** cost function

Strategy 6: the optimal use of prevention from human to human, isolation, and treatment only

Figure 7 illustrates the impact of the best use of human-to-human transmission prevention u_2, isolation of infected individuals through contact tracing u_3, and treatment of isolated individuals u_4 only on the infected and isolated human population. We also display the intervention's control profile and the associated cost function necessary for the intervention's successful effects on the human population. Figure 7A shows that, even when the triple intervention is used to its fullest potential, the number of infected people does not drop significantly (strategy 6). With this intervention, a total of 1.74×10^7 infected individuals were averted. It is very important to note that even though we implement triple control intervention, the total size of infected individuals averted is minimal. This result is likely due to the relaxation of the isolation intervention strategy u_3 as seen in the control profile Fig. 7C. The result of the combined interventions (strategy 6) on the isolated human population is similar to the outcome presented in Fig. 6B (see Sect. 5.5). The cost function for the triple interventions (strategy 6) is shown in Fig. 7D.

Strategy 7: the optimal use of all the controls

In Fig. 8A, B, we simulate the impact of all the combination strategies (optimal use of preventive strategies from rodents to humans u_1, prevention from human-to-human u_2, isolation of infected individuals through contact tracing u_3, and treatment of infected individuals u_4) on the infected and isolated humans population. Figure 8C is the control profile The result of this combined interventions (strategy 7) on the infected human population is similar to the result presented in Fig. 2A, 5A and 6A (see Sects. 5.1 and 5.5). However, it is worth noting that this intervention (strategy 7) averted a total size of 7.35×10^7 infected individuals. Also, the impact of strategy 7 on the isolated human population is similar to the result presented in Fig. 7B (see Sect. 5.6). In

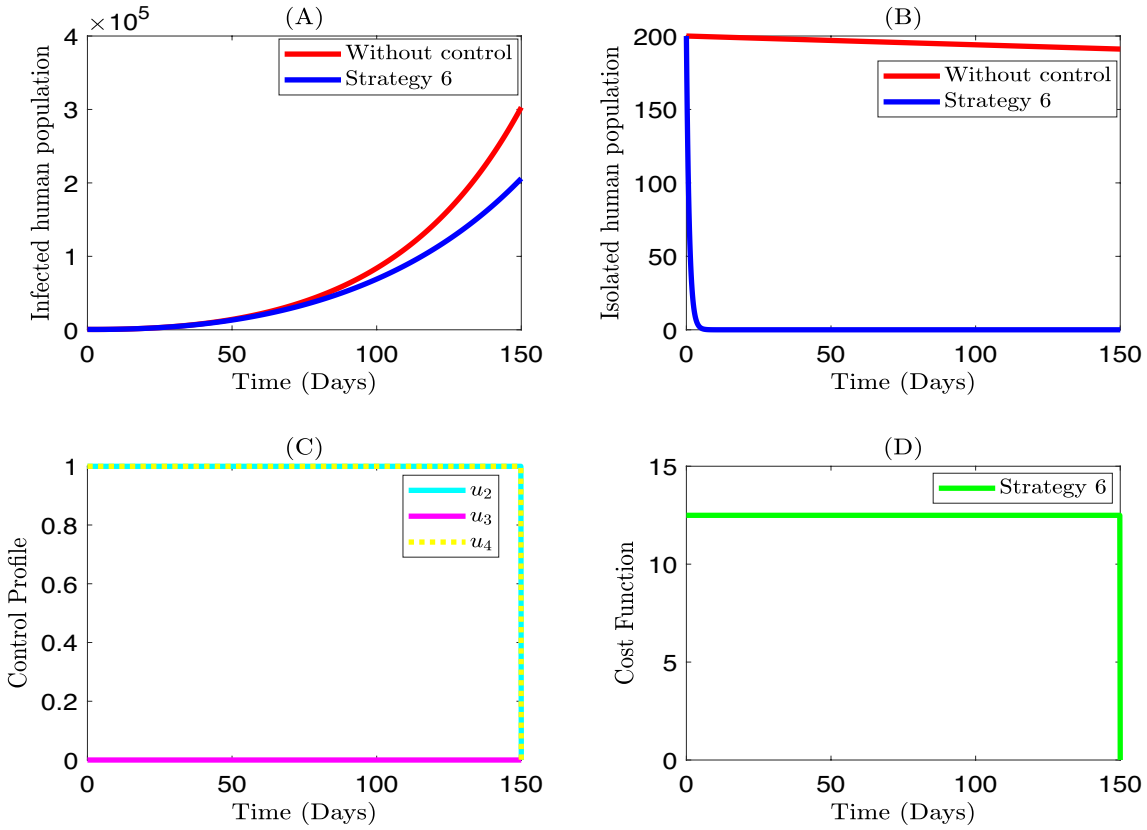

Fig. 7 Simulations of the effects of strategy 6 on the optimal control model. **A** Infected human population; **B** isolated human population; **C** control profile; and **D** cost function

Fig. 8D, the cost function of the combined interventions (strategy 7) is depicted.

Cost-effectiveness analysis

The cost and severity of disease mitigation are well known, especially in densely populated and low-income areas. Therefore, it is crucial to research the most cost-effective yet accessible control strategies that can be used to lessen the impact of monkeypox in a given population. The cost-effectiveness analysis is used in this section to investigate the most cost-effective control strategy among all the combinations of control strategies (scenario A to scenario D). We employed three different strategies namely; the infection averted ratio (IAR), average cost-effectiveness ratio (ACER), and incremental cost-effectiveness ratio (ICER), to accomplish this goal, as described in Ojo and Goufo (2022a) and Agusto and Leite (2019). In the sections that follow, we outline each methodology and the estimates it provides for the control strategies.

Infection averted ratio (IAR)

The ratio of individuals who recovered from an infection as a result of the intervention to the number of infections prevented by the intervention is known as the infection averted ratio (IAR). This is estimated as

$$\text{IAR} = \frac{\text{Number of infections averted}}{\text{Number of recovered individuals from the infection}}. \tag{17}$$

It is worth mentioning that the number of infections averted (IA) is determined by comparing the total infectious individuals under optimal control to the total infected individuals under no control. According to Ojo and Goufo (2022a) and Agusto and Leite (2019), the approach with the highest infection avoided ratio will be the most cost-effective in stopping the disease's spread among the populace. Table 4 lists the estimations of the total cost of control, IA, ACER, and IAR for the seven techniques taken into consideration in this study, while Fig. 9 depicts the IAR bar plots of scenario A, scenario B, and scenario C. According to the decision rule of IAR, the strategy with the highest ratio is the most cost-effective. Thus, the most cost-effective

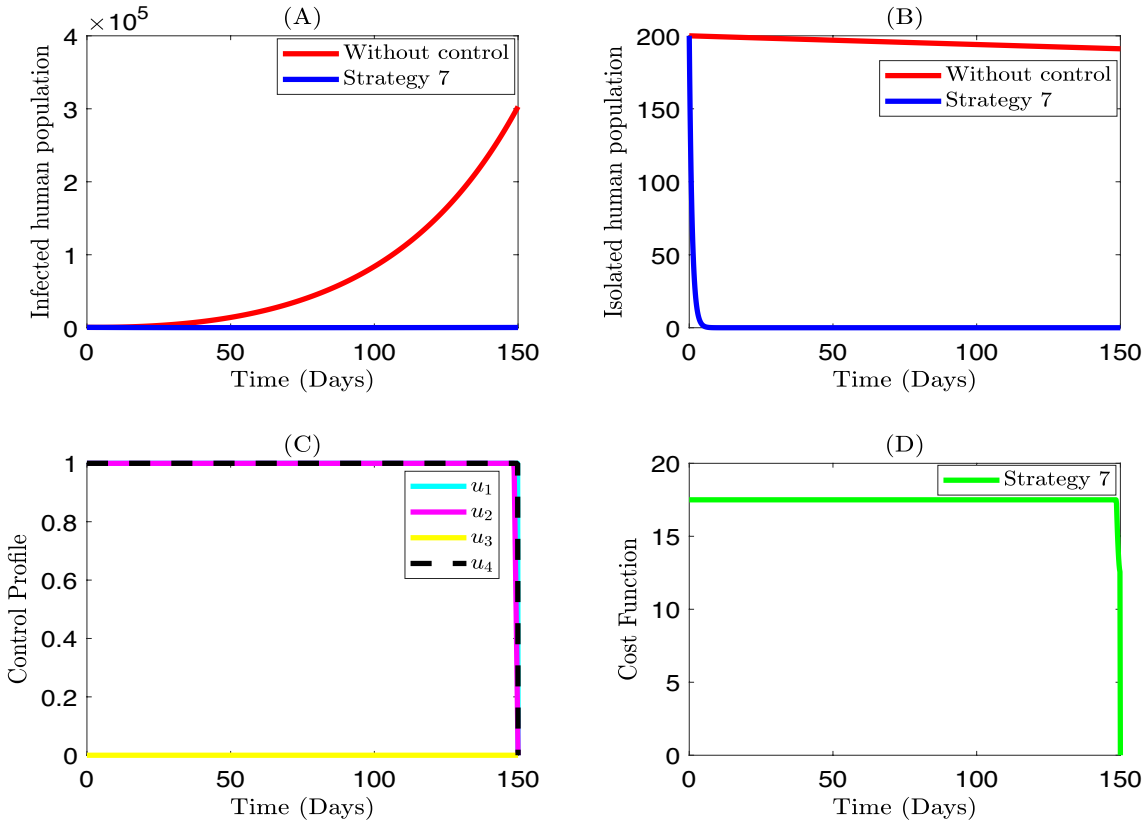

Fig. 8 Simulations of the effects of strategy 7 on the optimal control model. **A** Infected human population; **B** isolated human population; **C** control profile; and **D** cost function

Table 4 Total infection averted, total cost, ACER, and IAR for the intervention strategies of all scenarios

Scenarios	Strategies	Infection averted	Total cost	ACER	IAR
Scenario A	1	1.7268×10^7	5000	0.6879×10^{-4}	46.6207
	2	1.7168×10^7	4998	2.9110×10^{-4}	0.2087
Scenario B	3	6.5027×10^7	14674	2.2566×10^{-4}	0.4619
	4	7.3325×10^7	9979	1.3609×10^{-4}	119.7684
Scenario C	5	7.3659×10^7	13438	1.8244×10^{-4}	65.755
	6	1.7362×10^7	12494	7.1962×10^{-4}	0.2106
Scenario D	7	7.3519×10^7	17472	2.3765×10^{-4}	91.1558

strategies in scenario A, scenario B, and scenario C are strategy 1, strategy 4, and strategy 5, respectively. The most cost-effective strategy among those in scenarios A, through scenario C, is examined in the following subsection using the average cost-effectiveness ratio approach.

Average cost-effectiveness ratio (ACER)

The average cost-effectiveness ratio (ACER), which measures the effectiveness of a particular intervention strategy, is the ratio between the total cost incurred and the total number of infections prevented by that strategy. This is calculated by

$$\text{ACER} = \frac{\text{Total cost incurred by implementation of intervention}}{\text{Total number of infections averted by the intervention}}. \quad (18)$$

Notably, the objective function provided in (10) can be used to estimate the numerator of Eq. (18). A single optimal strategy is measured using ACER against a no-intervention scenario. The estimates of the ACER for the seven strategies considered in this study are tabulated in Table 4, while Fig. 10 depicts the ACER bar plots of scenario A, scenario B, and scenario C. The most cost-effective strategies in scenarios A through scenario C, according to the average cost-effective ratio method, are strategy 1, strategy 4, and

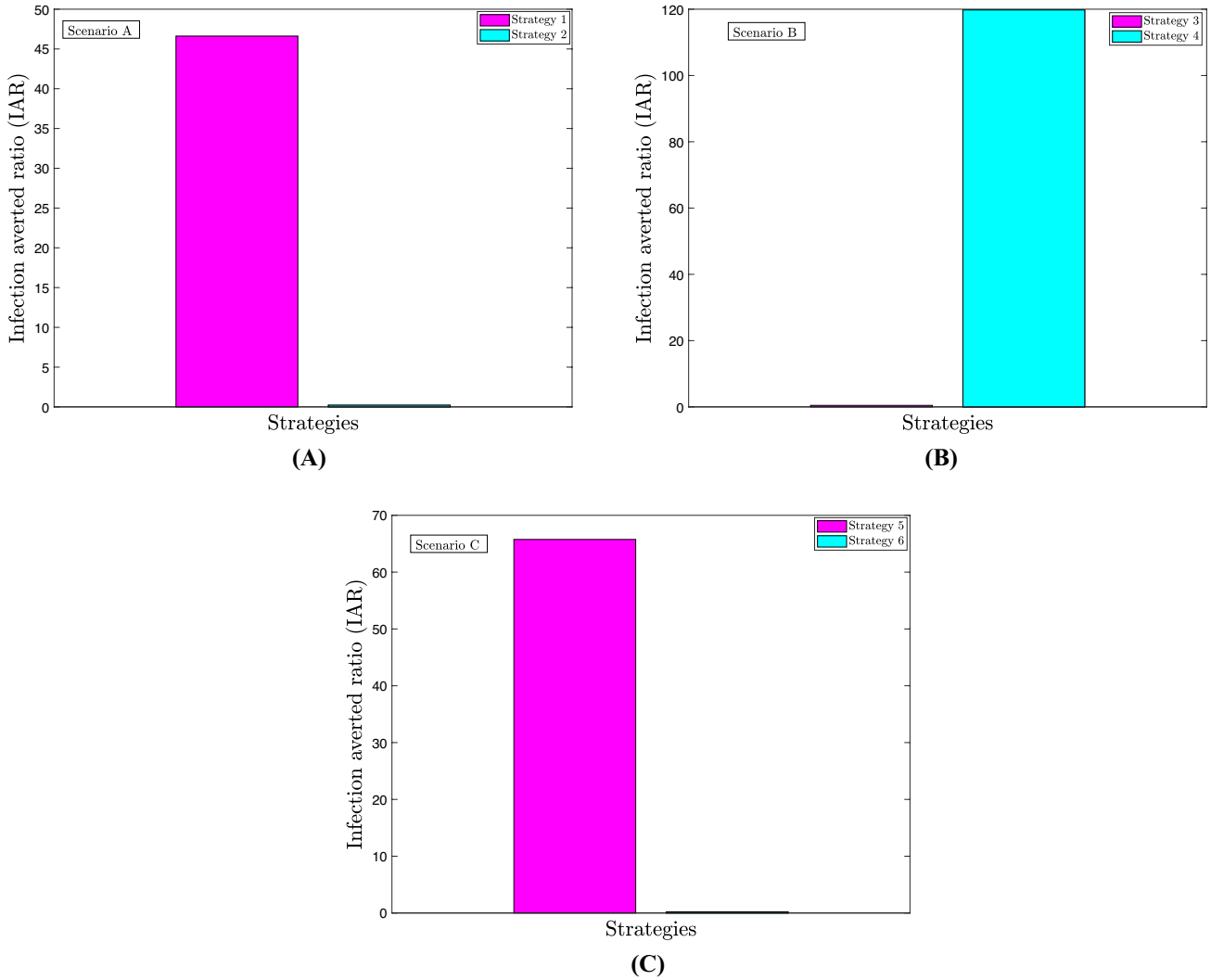

Fig. 9 Infection averted ratio for scenario A, B, and C

strategy 5, respectively. This outcome validates the one obtained by applying the infection averted ratio method.

Incremental cost-effectiveness ratio (ICER)

In this section, we investigate the most cost-effective strategy among all the strategies in scenarios A to C using the incremental cost-effectiveness ratio approach. The difference between two or more competing strategies, with their associated health benefits and implementation costs, is determined using the ICER. This is calculated by

$$\text{ICER} = \frac{\text{Difference in total costs between control strategies}}{\text{Difference in total infection averted by control strategies}}. \tag{19}$$

In the sections that follow, we will talk about how to estimate each strategy for its respective scenarios.

Scenario A

We present the monkeypox infection averted, the total cost of implementation, ACER, and ICER in Table 5 in increasing order of the infected averted in order to determine the most cost-effective strategy in scenario A (strategy 1 and strategy 2). The ICER's derivation is provided as follows:

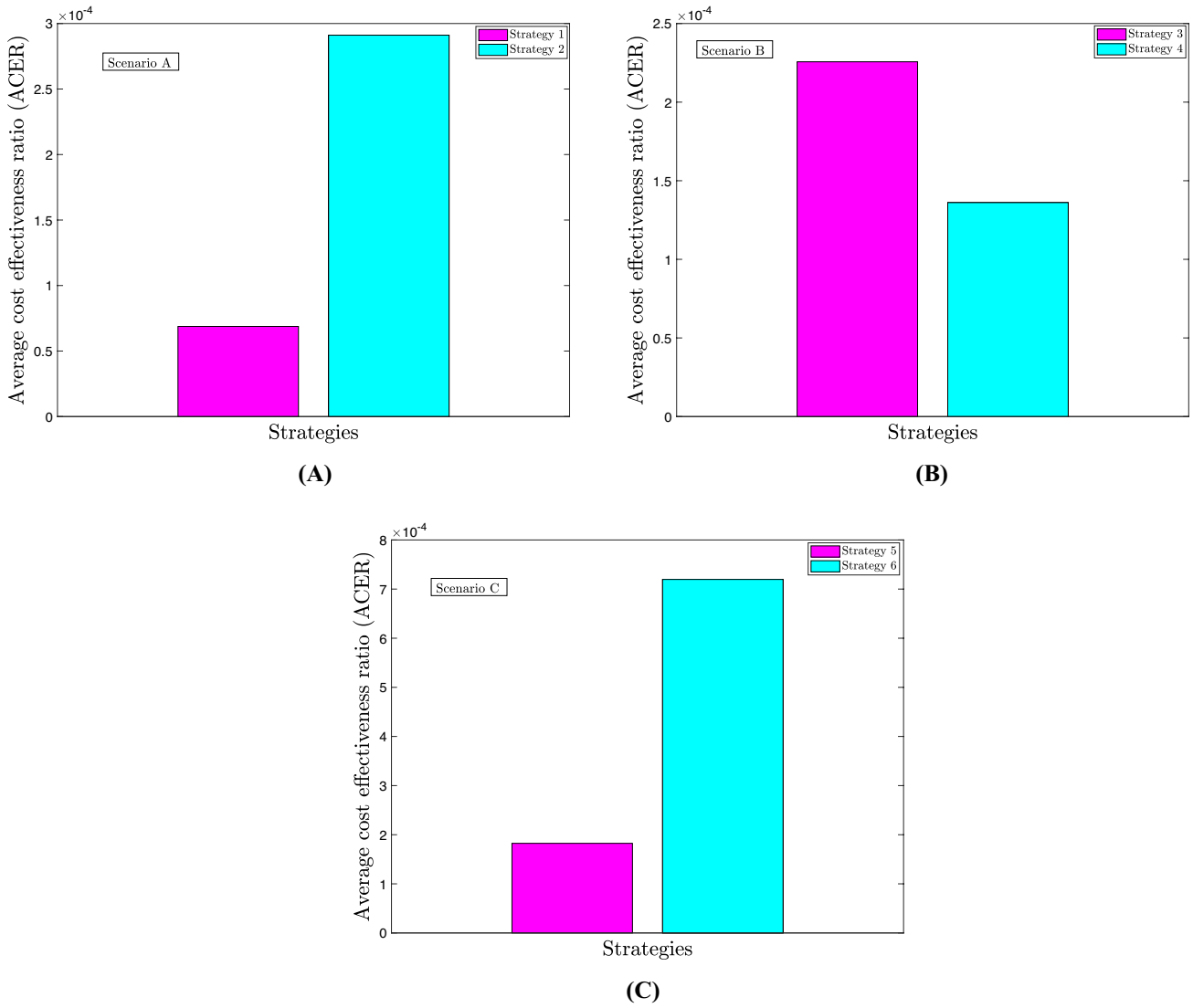

Fig. 10 ACER for scenario A, B, and C

Table 5 ICER for strategies 1 and 2

Strategies	IA ($\times 10^7$)	Total cost	ACER ($\times 10^{-4}$)	ICER
2	1.7168	4998	2.9110	2.9109×10^{-4}
1	7.2682	5000	0.6879	4.3232×10^{-8}

$$\text{ICER}(2) = \frac{4998}{(1.7168) \times 10^7} = 2.9109 \times 10^{-4}$$

$$\text{ICER}(1) = \frac{50000 - 4998}{(7.2682 - 1.7168) \times 10^7} = 4.3232 \times 10^{-8}.$$

We compare strategy 1 and strategy 2 and we observed a cost-saving of 2.9109×10^{-4} over strategy 1. We can see that ICER(2) exceeds ICER(1). This suggests that strategy 2 surpasses the other, proving that strategy 1 is the less expensive of the two strategies in scenario A. Therefore, strategy 1 is the most cost-effective in scenario A.

Table 6 ICER for strategies 3 and 4

Strategies	IA ($\times 10^7$)	Total cost	ACER ($\times 10^{-4}$)	ICER
3	6.5027	14674	2.2566	2.2566×10^{-4}
4	7.3325	9979	1.3609	-5.6580×10^{-4}

Scenario B

Among the double control strategies (strategy 3 and strategy 4), we examine which is the most economical. The cost of implementation, the infection prevented, the

Table 7 ICER for strategies 5 and 6

Strategies	IA ($\times 10^7$)	Total cost	ACER ($\times 10^{-4}$)	ICER
6	1.7362	12494	7.1962	7.1962×10^{-4}
5	7.3659	13438	1.8244	1.6768×10^{-5}

Table 8 ICER for strategies 1, 4, 5, and 7

Strategies	IA ($\times 10^7$)	Total cost	ACER ($\times 10^{-4}$)	ICER
1	7.2682	5000	0.6879	6.8793×10^{-5}
4	7.3325	9979	1.3609	7.7434×10^{-3}
7	7.3519	17472	2.3765	3.8624×10^{-2}
5	7.3659	13438	1.8244	-2.8814×10^{-2}

ACER, and the ICER are all given in Table 6. The ICER calculation is provided as follows:

$$\text{ICER}(3) = \frac{14674}{(6.5027) \times 10^7} = 2.2566 \times 10^{-4}$$
$$\text{ICER}(4) = \frac{9979 - 14674}{(7.3325 - 6.5027) \times 10^7} = -5.6580 \times 10^{-4}.$$

Since ICER(3) > ICER(4), this implies that strategy 4 is the most cost-efficient among the two strategies in scenario B.

Scenario C

We examine the most cost-effective strategy among the triple control strategies (strategy 5 and strategy 6). The infection averted, cost of implementation, ACER, and the ICER are tabulated in Table 7. The calculation of the ICER is given as follows:

$$\text{ICER}(6) = \frac{12494}{(1.7362) \times 10^7} = 7.1962 \times 10^{-4}$$
$$\text{ICER}(5) = \frac{13438 - 12494}{(7.3659 - 1.7362) \times 10^7} = 1.6768 \times 10^{-5}.$$

Since ICER(6)>ICER(5), this implies that strategy 5 is the most cost-efficient among the two strategies in scenario C.

All the most cost-effective strategies from all scenarios

We looked at the most economical approaches in each case in the sections before using various techniques. We observe that in scenario A, scenario B, and scenario C, respectively, all the methodologies used selected strategy 1, strategy 4, and strategy 5 as the most cost-effective strategies. We now choose strategies 1, 4, and 5 (which are the chosen strategies from scenarios A through C) and strategy 7 to analyze the overall minimal cost strategy among all the techniques in this study. Table 8 lists the infection avoided, implementation costs, ACER, and ICER. From Table 8, we compare strategy 1 and strategy 4, and it was noted that ICER(4)>ICER(1). This informs us that strategy 1 is less costly and more efficient when compared to strategy 4. As a result, we eliminate strategy 4, to further our investigation with the remaining alternative strategies. The infection averted, cost of implementation, ACER, and the ICER of the remaining competing strategies are given in Table 9.

Table 9 ICER for strategies 1, 5, and 7

Strategies	IA ($\times 10^7$)	Total cost	ACER ($\times 10^{-4}$)	ICER
1	7.2682	5000	0.6879	6.8793×10^{-5}
7	7.3519	17472	2.3765	1.4901×10^{-2}
5	7.3659	13438	1.8244	-2.8814×10^{-2}

Table 10 ICER for strategies 1 and 5

Strategies	IA ($\times 10^7$)	Total cost	ACER ($\times 10^{-4}$)	ICER
1	7.2682	5000	0.6879	6.8793×10^{-5}
5	7.3659	13438	1.8244	8.6366×10^{-3}

We compare strategy 1 with strategy 7 in Table 9 and find that ICER(7)>ICER (1). This shows us that strategy 1 is more effective and less expensive than strategy 7 overall. In order to continue our analysis with the remaining potential tactics, we, therefore, discard strategy 7. Table 10 lists the infections avoided, implementation costs, ACERs, and ICERs of the remaining competing options. From Table 10, strategy 1 and strategy 5 were compared, and it was noted that ICER(5)>ICER(1). This shows us that, compared to strategy 5, strategy 1 is less expensive and more effective. Therefore, among all other strategies in this study, the implementation of preventive strategies for transmission of infection from rodents to humans to stop transmission between the rodent and human populations (strategy 1) is considered to be the most cost-effective strategy.

Conclusion and recommendations

Multiple interventions are required to reduce the ongoing incidence of monkeypox since the prevalence poses a threat to the human population. To gain more insight into the spread and control of monkeypox disease in the communities, we develop and analyzed a mathematical model to investigate the impact of various control mechanisms that can be used to lessen the disease burden. In Sect. 2, we present and analyzed the basic model without optimal control variables (1). The threshold quantity known as the reproduction number was obtained and used to examine the model's local and

global stability. The outcome demonstrates that when the reproduction number $\mathcal{R}_0 < 1$, the model's disease-free equilibrium would be locally and globally asymptotically stable. To investigate the impact of various optimum control strategies on the reduction of the ongoing monkeypox prevalence, we extended the basic model (1) by incorporating four time-dependent control variables. These controls are preventive strategies for transmission from rodents to humans u_1, prevention of infection from human to human u_2, isolation of infected individuals u_3, and treatment of isolated individuals u_4.

The renowned Pontryagin's maximal principle technique was used to find the optimal solutions. We simulate the dynamics of the infected and isolated human populations using the fourth-order Runge–Kutta forward–backward sweep method to show how each intervention strategy affects the burden of monkeypox. Each control strategy effectively lessens the burden of the infected population when compared to the case without control, as shown in Fig. 2 through Fig. 8. It should be noted that among all the competing strategies, strategy 7 (the combination of all the strategies), has the highest size of infected human averted (7.3519×10^7). Implementing the combination of all four strategies would help reduce the burden of monkeypox, especially in a critical phase of the disease insurgence. However, this can be very expensive, especially for high populated and low-income nations. Because of this, we performed a cost-effectiveness analysis using the infection averted ratio (IAR), average cost-effective ratio (ACER), and the incremental cost-effectiveness ratio (ICER) method, to determine the most cost-effective strategies that can be used in reducing monkeypox infections. The overall conclusion of this analysis shows that implementing preventive strategies (strategy 1) for transmission from rodents to humans is the most economical and effective among all competing strategies.

Based on the findings of this study, we advise health policy decision-makers to expand public health initiatives to educate people about preventive measures that can be taken to stop the spread of infection from rodents to humans. Examples of these include maintaining good personal hygiene, avoiding close contact with bodily fluids or animal rashes caused by monkeypox, and making sure that animals are properly cooked to prevent the consumption of infected animals. The Centers for Disease Control and Prevention (CDC) also advocated for this course of action (Centers for Disease Control and Prevention 2022b; Mayo Clinic 2022). The current model can be extended to account for the vaccination of susceptible individuals in order to further investigate the impact of vaccine usage. With the aid of the model, it is possible to investigate the effects of widespread vaccination against monkeypox on the suppression of the disease's insurgence.

Data Availability Data used to support the findings of this study are included in the article. The authors used a set of parameter values whose sources are from the literature as shown in Table 1.

Declarations

Conflict of interest The authors declare that they have no known competing financial interests or personal relationships that could have appeared to influence the work reported in this paper.

References

Abioye A, Ibrahim M, Peter O, Amadiegwu S, Oguntolu F (2018) Differential transform method for solving mathematical model of SEIR and SEI spread of malaria 40(1):197–219

Abioye AI, Peter OJ, Ogunseye HA, Oguntolu FA, Oshinubi K, Ibrahim AA, Khan I (2021) Mathematical model of Covid-19 in Nigeria with optimal control. Results Phys 28:104598

Agusto F, Leite M (2019) Optimal control and cost-effective analysis of the 2017 meningitis outbreak in Nigeria. Infect Dis Model 4:161–187

Alakunle E, Moens U, Nchinda G, Okeke M (2020) Monkeypox virus in Nigeria: infection biology, epidemiology, and evolution. Viruses 12(11):1257

Ayoola TA, Edogbanya HO, Peter OJ, Oguntolu FA, Oshinubi K, Olaosebikan ML (2021) Modelling and optimal control analysis of typhoid fever. J Math Comput Sci 11(6):6666–6682

Bankuru SV, Kossol S, Hou W, Mahmoudi P, Rychtář J, Taylor D (2020) A game-theoretic model of monkeypox to assess vaccination strategies. PeerJ 8:e9272

Bhunu C, Mushayabasa S (2011) Modelling the transmission dynamics of pox-like infections. IAENG Int J 41(2):1–9

Bhunu C, Garira W, Magombedze G (2009) Mathematical analysis of a two strain hiv/aids model with antiretroviral treatment. Acta Biotheoretica 57(3):361–381

Bisanzio D, Reithinger R (2022) Projected burden and duration of the 2022 monkeypox outbreaks in non-endemic countries. The Lancet, Microbe

Center for Disease Control (2022) Interim clinical guidance for the treatment of monkeypox. https://www.cdc.gov/poxvirus/monkeypox/index.html/. Accessed 20 May 2022

Centers for Disease Control and Prevention (2022a) Monkeypox—how to protect yourself. https://www.cdc.gov/poxvirus/monkeypox/prevention/protect-yourself.html. Accessed 30 July 2022

Centers for Disease Control and Prevention (2022b) Prevention of monkeypox. https://www.cdc.gov/poxvirus/monkeypox/prevention.html. Accessed 31 July 2022

Choi SK, Kang B, Koo N (2014) Stability for Caputo fractional differential systems. In: Abstract and applied analysis, volume 2014. Hindawi

Durski KN, McCollum AM, Nakazawa Y, Petersen BW, Reynolds MG, Briand S, Djingarey MH, Olson V, Damon IK, Khalakdina A (2018) Emergence of monkeypox-west and central Africa, 1970–2017. Morb Mortality Wkly Rep 67(10):306

Emeka P, Ounorah M, Eguda F, Babangida B (2018) Mathematical model for monkeypox virus transmission dynamics. Epidemiol Open Access 8(3):1000348

Fleming WH, Rishel RW (2012) Deterministic and stochastic optimal control, vol 1. Springer, New York

Grant R, Nguyen L-BL, Breban R (2020) Modelling human-to-human transmission of monkeypox. Bull World Health Organ 98(9):638

Jezek Z, Szczeniowski M, Paluku K, Mutombo M, Grab B (1988) Human monkeypox: confusion with chickenpox. Acta Tropica 45(4):297–307

Lasisi N, Akinwande N, Oguntolu F (2020) Development and exploration of a mathematical model for transmission of monkeypox disease in humans. Math Models Eng 6(1):23–33

Madubueze CE, Gweryina RI, Tijani KA (2021) A dynamic model of typhoid fever with optimal control analysis. Ratio Mathematica 41:255

Mayo Clinic (2022) Monkeypox: What is it and how can it be prevented? https://www.mayoclinic.org/diseases-conditions/infectious-diseases/expert-answers/monkeypox-faq/faq-20533608. Accessed 31 July 2022

Ojo MM, Goufo EFD (2021) Assessing the impact of control interventions and awareness on malaria: a mathematical modeling approach. Commun Math Biol Neurosci 2021

Ojo MM, Goufo EFD (2022a) Mathematical analysis of a lassa fever model in nigeria: optimal control and cost-efficacy. Int J Dyn Control 1–22

Ojo MM, Goufo EFD (2022b) Modeling, analyzing and simulating the dynamics of Lassa fever in Nigeria. J Egypt Math Soc 30(1):1–31

Ojo M, Gbadamosi B, Olukayode A, Oluwaseun OR (2018) Sensitivity analysis of dengue model with saturated incidence rate. Open Access Libr J 5(03):1

Ojo MM, Gbadamosi B, Benson TO, Adebimpe O, Georgina A (2021) Modeling the dynamics of Lassa fever in Nigeria. J Egypt Math Soc 29(1):1–19

Ojo MM, Benson TO, Peter OJ, Goufo EFD (2022a) Nonlinear optimal control strategies for a mathematical model of covid-19 and influenza co-infection. Physica A Stat Mech Appl 607:128173

Ojo MM, Benson TO, Shittu AR, Doungmo Goufo EF (2022b) Optimal control and cost-effectiveness analysis for the dynamic modeling of Lassa fever. J Math Comput Sci 12

Ojo MM, Peter OJ, Goufo EFD, Panigoro HS, Oguntolu FA (2022) Mathematical model for control of tuberculosis epidemiology. J Appl Math Comput 1–19

Peter O, Ibrahim M, Oguntolu F, Akinduko O, Akinyemi S (2018) Direct and indirect transmission dynamics of typhoid fever model by differential transform method

Peter OJ, Viriyapong R, Oguntolu FA, Yosyingyong P, Edogbanya HO, Ajisope MO (2020) Stability and optimal control analysis of an SCIR epidemic model. J Math Comput Sci 10(6):2722–2753

Peter OJ, Kumar S, Kumari N, Oguntolu FA, Oshinubi K, Musa R (2021a) Transmission dynamics of monkeypox virus: a mathematical modelling approach. Model Earth Syst Environ 1–12

Peter OJ, Qureshi S, Yusuf A, Al-Shomrani M, Idowu AA (2021b) A new mathematical model of covid-19 using real data from Pakistan. Results Phys 24:104098

Peter OJ, Oguntolu FA, Ojo MM, Olayinka A, Jan R, Khan I (2022) Fractional order mathematical model of monkeypox transmission dynamics. Physica Scripta

Pontryagin LS (1987) Mathematical theory of optimal processes. CRC Press, Boca Raton

Somma S, Akinwande N, Chado U (2019) A mathematical model of monkey pox virus transmission dynamics. Ife J Sci 21(1):195–204

TeWinkel RE (2019) Stability analysis for the equilibria of a monkeypox model. Thesis and Dissertations: University of Wisconsin. https//dc.uwm.edu/etd/2132. Accessed 20 May 2022

Usman S, Adamu II et al (2017) Modeling the transmission dynamics of the monkeypox virus infection with treatment and vaccination interventions. J Appl Math Phys 5(12):2335